## 1. Experimental section

### 1.1. Materials and apparatus

10-Phenanthrolin-5-amine, $Ru(bpy)_3Cl_2$, Cholic acid, EDC·HCl, and NHS were purchased from Energy Chemical (China). DMSO, MTT, DCFH-DA, and the Annexin V apoptosis detection kit were purchased from Sigma Aldrich (USA). ER-Tracker Red was purchased from Beyotime (China). The antibodies were obtained from Cell Signaling Technology (USA) and used as recommended by the manufacturer. The BALB/c mice were purchased from Guangdong Provincial Medical Laboratory Animal Center (China).

$^1$H NMR spectra of the compounds were obtained in DMSO-$d_6$ on a Bruker AVANCE 400/600 spectrometer (Germany). ESI-MS spectra of the compounds were obtained on a Shimadzu LCMS-2020 spectrometer (Japan). Absorption and emission spectra were obtained using a Cary 60 spectrophotometer and a Hitachi F-7000 fluorescence spectrophotometer, respectively. A blue-violet LED array ($\lambda_{ir}$ = 450 nm, 15 mW cm$^{-2}$) was used for light irradiation experiments. Confocal microscopic images were acquired using a Leica TCS SP8 confocal microscope (Germany). Flow cytometry was conducted on a BD FACS Calibur flow cytometer (USA).

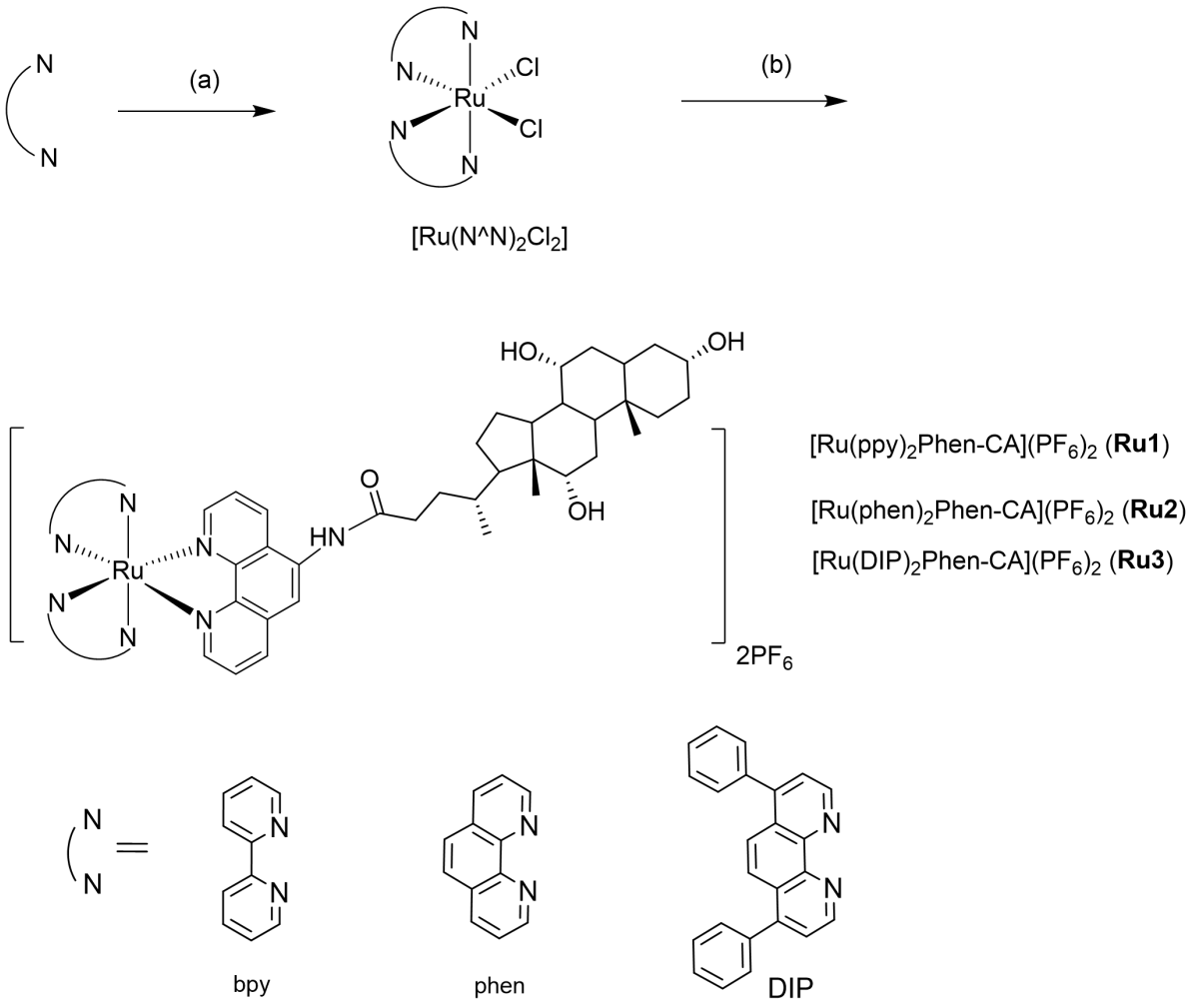


**Scheme S1.** Synthetic routes of **Ru1**-**Ru3**. (a) $RuCl_3$, bpy, phen or DIP, DMF. (b) **Phen-CA**, methanol and $H_2O$.

**1.2. Synthesis of the complexes Ru1-Ru3**

The precursors of cis-$[Ru(bpy)_2Cl_2]\cdot 2H_2O$[1], cis-$[Ru(phen)_2Cl_2]\cdot 2H_2O$[2], cis-$[Ru(DIP)_2Cl_2]\cdot 2H_2O$[3]and ligand **Phen-CA**[4] were prepared according to literature procedures. The synthetic routes of **Ru1**-**Ru3** are shown in Scheme S1. **$Ru(N\hat{}N)_2Cl_2$** (0.50 mmol) and **Phen-CA** (0.50 mmol) were refluxed in $CH_3CH_2OH$ for 12 h under nitrogen. After that, the solvent was concentrated under vacuum and a red precipitate was obtained by the dropwise addition of saturated $NH_4PF_6$ aqueous solution. Then, the crude product was purified by silica gel column chromatography with an acetonitrile : water : saturated potassium nitrate (100 : 9 : 1, v/v/ v) mobile phase[5]. The $PF_6$ salts of **Ru1**-**Ru3** were again formed by adding saturated $NH_4PF_6$ aqueous solution, and then dried under vacuum.

$[Ru(bpy)_2(Phen\text{-}CA)](PF_6)_2$ (**Ru1**) is an orange solid with a yield of 69% (0.34 mmol, 437.37 mg). $^1$H NMR (400 MHz, DMSO) δ 10.49 (s, 1H), 8.95 (d, *J* = 8.4 Hz, 1H), 8.88 (d, *J* = 8.2 Hz, 2H), 8.84 (d, *J* = 8.2 Hz, 2H), 8.74 (d, *J* = 8.2 Hz, 1H), 8.66 (s, 1H), 8.25 – 8.19 (m, 2H), 8.16 (d, *J* = 5.1 Hz, 1H), 8.11 (dt, *J* = 7.6, 3.9 Hz, 2H), 8.03 (d, *J* = 5.2 Hz, 1H), 7.92 (dd, *J* = 8.4, 5.4 Hz, 1H), 7.87 – 7.81 (m, 3H), 7.59 (dt, *J* = 11.2, 5.8 Hz, 4H), 7.37 (t, *J* = 6.5 Hz, 2H), 4.35 (s, 1H), 4.17 (s, 1H), 4.03 (s, 1H), 3.84 (s, 1H), 3.63 (s, 1H), 3.19 (d, *J* = 21.4 Hz, 1H), 2.69 – 2.60 (m, 1H), 2.57 – 2.52 (m, 1H), 2.29 – 2.13 (m, 2H), 2.08 – 1.99 (m, 1H), 1.94 – 1.75 (m, 4H), 1.65 (dd, *J* = 17.1, 14.2 Hz, 2H), 1.51 – 1.19 (m, 11H), 1.10 – 0.95 (m, 4H), 0.90 – 0.79 (m, 4H), 0.63 (s, 3H). $^{13}$C NMR (400 MHz, DMSO) δ 173.74 (s), 157.27 (s), 157.02 (d, *J* = 3.6 Hz), 152.73 (s), 151.89 (d, *J* = 10.1 Hz), 151.47 (s), 147.67 (s), 144.90 (s), 138.36 (d, *J* = 18.5 Hz), 136.72 (s), 134.46 (s), 133.15 (s), 130.76 (s), 128.25 (d, *J* = 13.8 Hz), 126.96 (s), 126.81 (s), 126.16 (s), 124.89 (d, *J* = 12.4 Hz), 119.56 (s), 71.50 (s), 70.88 (s), 66.71 (s), 46.57 (s), 46.24 (s), 41.94 (d, *J* = 6.4 Hz), 35.73 (d, *J* = 10.4 Hz), 35.39 (s), 34.87 (s), 33.48 (s), 31.89 (s), 30.87 (s), 29.08 (s), 27.81 (s), 26.72 (s), 23.30 (s), 23.10 (s), 17.68 (d, *J* = 1.3 Hz), 12.86 (s). ESI-MS (MeOH): *m*/*z* 499.6977 $[M-2PF_6]^{2+}$. Purity > 97% (by HPLC).

$[Ru(phen)_2(Phen\text{-}CA)]$ $(PF_6)_2$ (**Ru2**) is a red solid with a yield of 78% (0.39 mmol, 520.41 mg). $^1$H NMR (400 MHz, DMSO) δ 10.48 (s, 1H), 8.92 (d, *J* = 8.6 Hz, 1H), 8.80 – 8.68 (m, 5H), 8.65 (s, 1H), 8.39 (s, 4H), 8.13 – 8.02 (m, 5H), 7.96 (dd, *J* = 5.2, 1.1 Hz, 1H), 7.83 – 7.73 (m, 5H), 7.70 (dd, *J* = 8.3, 5.3 Hz, 1H), 4.33 (d, *J* = 3.9 Hz, 1H), 4.15 (d, *J* = 2.7 Hz, 1H), 4.01 (d, *J* = 3.3 Hz, 1H), 3.83 (s, 1H), 3.62 (s, 1H), 3.18 (dd, *J* = 12.1, 4.7 Hz, 1H), 2.70 – 2.58 (m, 1H), 2.20 (dt, *J* = 24.6, 12.2 Hz, 2H), 2.02 (dd, *J* = 19.1, 11.9 Hz, 1H), 1.94 – 1.72 (m, 4H), 1.65 (d, *J* = 12.0 Hz, 2H), 1.50 – 1.15 (m, 12H), 1.10 – 0.94 (m, 4H), 0.92 – 0.76 (m, 4H), 0.62 (s, 3H). $^{13}$C NMR (151 MHz, DMSO) δ 172.70 (s), 152.15 (s), 150.92 (s), 146.99 (s), 146.59 (s), 144.24 (s), 136.23 (s), 135.60 (s), 133.35 (s), 132.09 (s), 129.84 (s), 127.45 (s), 125.75 (s), 124.94 (s), 118.54 (s), 70.42 (s), 69.79 (s), 65.62 (s), 62.18 (s), 45.51 (s), 45.16 (s), 40.87 (s), 34.66 (d, *J* = 7.4 Hz), 34.31 (s), 33.78 (s), 32.42 (s), 30.85 (s), 29.78 (s), 28.00 (s), 26.74 (s), 25.63 (s), 22.22 (s), 22.02 (s), 16.60 (s), 11.78 (s). ESI-MS (MeOH): *m*/*z* 523.6976 $[M-2PF_6]^{2+}$. Purity > 96% (by HPLC).

$Ru(DIP)_2(Phen\text{-}CA)]$ $(PF_6)_2$ (**Ru3**) is a red solid with a yield of 76% (0.38 mmol, 623.02 mg).$^1$H NMR (400 MHz, DMSO) δ 10.51 (s, 1H), 8.96 (d, *J* = 8.3 Hz, 1H), 8.79 (d, *J* = 7.7 Hz, 1H), 8.67 (s, 1H), 8.40 – 8.30 (m, 2H), 8.27 (d, *J* = 5.4 Hz, 5H), 8.20 (d, *J* = 5.6 Hz, 2H), 8.14 (d, *J* = 4.3 Hz, 1H), 7.90 (dd, *J* = 8.5, 5.4 Hz, 1H), 7.85 – 7.75 (m, 5H), 7.70 – 7.59 (m, 19H), 4.33 (d, *J* = 4.1 Hz, 1H), 4.15 (d, *J* = 3.1 Hz, 1H),

4.01 (t, *J* = 2.9 Hz, 1H), 3.83 (s, 1H), 3.62 (s, 1H), 3.20 (s, 1H), 2.69 – 2.61 (m, 1H), 2.28 – 2.12 (m, 2H), 2.02 (dd, *J* = 18.9, 11.8 Hz, 1H), 1.84 (dd, *J* = 43.1, 8.5 Hz, 4H), 1.65 (d, *J* = 12.4 Hz, 2H), 1.35 (dd, *J* = 45.4, 36.3 Hz, 13H), 1.04 (t, *J* = 10.3 Hz, 4H), 0.83 (d, *J* = 11.9 Hz, 4H), 0.62 (s, 3H). $^{13}$C NMR (400 MHz, DMSO) δ 172.72 (s), 151.91 (s), 151.58 (s), 147.42 (d, *J* = 12.2 Hz), 146.96 (s), 144.25 (s), 134.82 (d, *J* = 7.0 Hz), 133.39 (s), 129.31 (s), 129.08 (s), 128.56 (s), 127.55 (s), 125.87 (s), 125.41 (s), 70.42 (s), 69.79 (s), 65.62 (s), 45.50 (s), 45.16 (s), 40.87 (s), 40.73 (s), 34.63 (s), 34.32 (s), 33.78 (s), 30.86 (s), 29.78 (s), 28.02 (s), 26.74 (s), 25.64 (s), 22.22 (s), 22.02 (s), 16.61 (s), 11.79 (s). ESI-MS (MeOH): *m*/*z* 675.7612 $[M-2PF_6]^{2+}$. Purity > 96% (by HPLC).

**1.3. Detection of $^1O_2$ generation**

The ability of complexes **Ru1**-**Ru3** to produce $^1O_2$ upon light irradiation was determined in DMSO according to the reported procedure with DPBF as the $^1O_2$ scavenger. The DMSO solutions containing DPBF (100 μM) and complexes **Ru1**-**Ru3** prepared in cuvettes were equilibrated with air. The absorbance of **Ru1**-**Ru3** in methanol at 450 nm was adjusted to about 0.15. The solution was then irradiated with a blue-violet LED light array ($\lambda_{ir}$ = 450 nm, 15 mW cm$^{-2}$) at room temperature. The absorption spectrum of DPBF in DMSO was recorded every 2 s of light irradiation.

**1.4. Cell lines and culture conditions**

The human breast cancer (MDA-MB-231) and mouse breast cancer (4T1) cells were obtained from the Experimental and Animal Centre of Sun Yat-sen University. Cells were maintained in Dulbecco's modified Eagle's medium (DMEM), which was supplemented with 10% fetal bovine serum (FBS), 100 μg/mL streptomycin and 100 U/mL penicillin, in a humidified incubator at 37 °C with 5% $CO_2$.

**1.5. Cellular localization studies**

The localization of **Ru1** in MDA-MB-231 cells was observed by confocal laser fluorescence microscopy. The cells cultured in 15 mm Corning culture dishes were treated with **Ru1** (10 μM) in DMEM at 37 °C for 4 h, and then incubated with ER-Tracker Red (1 μM) for 30 min. After the media was removed, the cells were rinsed three times with PBS and immediately observed with a Leica TCS SP8 confocal microscope. The excitation and emission wavelengths were set as follows: **Ru1**: Ex = 405 nm, Em = 550–650 nm; ER-Tracker Red: Ex = 633 nm, Em = 660–700 nm.

**1.6. PDT activity test**

The PDT activity of **Ru1**-**Ru3** in MDA-MB-231 cells and 4T1 cells was determined by the MTT method. The cells seeded onto 96-well culture plates were incubated at 37 °C for 24 h before treatment with **Ru1**-**Ru3**. Complexes **Ru1**-**Ru3** were diluted in DMSO to prepare a stock solution (20 mM), which was then diluted with culture medium to obtain medium solutions containing different concentrations of **Ru1**-**Ru3**. The final concentrations of DMSO in these medium solutions were kept at 1% (v/v). The cells were incubated with medium solutions containing different concentrations of **Ru1**-**Ru3** in darkness for 44 h. If light irradiation was needed, the cells were irradiated with a blue-violet LED light array ($\lambda_{ir}$ = 450 nm, 15 mW cm$^{-2}$) for 15 min after incubation for 12 h. Next, add 20 μL of MTT solution (5 mg mL$^{-1}$) to each well of the 96-well plate. After incubation at 37 °C for 4 h, the medium was removed from the culture plate and 150 μL DMSO was added to each well. After shaking the plate for 2 min, OD values at 595 nm were measured by a microplate reader. Cell viability was obtained from the ratio of the mean OD value of the dosed wells to the mean OD value of the control wells.

**1.7. ROS detection**

The ROS levels in MDA-MB-231 cells upon PDT treatment were measured by confocal microscopy using DCFH-DA as an indicator. Cells inoculated in 30 mm Corning cell culture dishes were exposed to **Ru1** (1.2 μM) for 12 h. Cells were stained with DCFH-DA (10 μM) for 20 min at 37 °C in the dark. Then the cells were irradiated with a blue-violet LED light array ($\lambda_{ir}$ = 450 nm, 15 mW cm$^{-2}$) for 0, 5, 10 and 15 min. Next, the cells were rinsed twice with PBS and analyzed by laser confocal microscopy immediately. $E_x$ = 488 nm and $E_m$ = 520 ± 20 nm for DCF.

### 1.8. Transmission electron microscopy

MDA-MB-231 cells were cultured in 10-cm dishes (Corning) and treated with **Ru1** (1.2 μM) for 12 h, followed by irradiation with a blue-violet LED light ($\lambda_{ir}$ = 450 nm, 15 mW $cm^{-2}$) for 15 min and further incubated in the dark for 12 h. The cells were rinsed with PBS and fixed overnight at 4 ℃ in a phosphate buffer containing 2.5% glutaraldehyde. After treatment with osmium tetroxide as post-fixative, the cells were stained with uranyl acetate and lead citrate, and then observed by a transmission electron microscope.

### 1.9. Western blotting

MDA-MB-231 cells were seeded into 6 cm cell culture dishes and incubated for 24 h. Cells were treated with complex **Ru1** (1.2 μM) for 12 h, then irradiated with a blue-violet LED light ($\lambda_{ir}$ = 450 nm, 15 mW $cm^{-2}$) for 0, 5, 10, and 15 min, respectively, and further incubated in the dark for 12 h. Cells were harvested and washed with ice-cold PBS twice, and then lysed in RIPA buffer supplemented with inhibitors of proteases and inhibitor of phosphatases sodium orthovanadate. The protein concentration was quantified using the BCA Protein Quantitation Kit. Equal amounts of cellular total proteins (30 μg) were separated on SDS-polyacrylamide gel electrophoresis and then transferred onto polyvinylidene difluoride membranes. Membranes were blocked in QuickBlock™ Blocking Buffer, and then incubated overnight with the primary antibodies CHOP, p-STAT3, γ-H2AX, GSDMD, GSDMD-N, p-STING, STING, p-$IRF_3$, $IRF_3$, p-$TBK_1$, $TBK_1$, p-NF-κB, NF-κB at 4 °C. After a subsequent washing step, the membrane was incubated with the appropriate horseradish peroxidase-conjugated secondary antibody. Images were captured using a FluorChem M imaging station and analyzed manually with AlphaView software.

### 1.10. Cellular immunofluorescence

According to the performance of HMGB1 and CRT on the surface of tumor cells, immunofluorescence (IF) analysis was employed to estimate ICD induced by **Ru1** *in vitro*. Specifically, $5\times10^4$ MDA-MB-231 cells were added to a confocal dish with a bottom dish diameter of 15 mm and incubated overnight, then treated with **Ru1** (1.2 μM) for 12 h, and then given different light times (0, 5, 10 and 15min). After rinsed with PBS, fixed, permeated and blocked in turns, then cultured with primary antibodies of anti-HMGB1 and anti-CRT at 4 °C overnight, cells were replaced with AF488-labeled secondary antibodies for 1 h and stained by Hoechst for 10 min, finally tested by CLSM. In another aspect, solid tumors of each group were sliced into sections for HMGB1 and CRT immunofluorescence detection. By way of deparaffinized, dehydrated, heat induced epitope retrieval with citrate buffer (pH = 6.0) and closure by 10% goat serum in 37 °C, tumor sections were separately incubated with primary and secondary antibodies, as same as the process of intracellular detection of CRT and HMGB1 *in vitro*. All immunofluorescence staining slices were scanned by CLSM.

### 1.11. Measurement of extracellular ATP levels

MDA-MB-231 cells were inoculated in a 2 cm culture dish, **Ru1** (1.2 μM) was added after 24 h, and after 12 h incubation, laser light (450 nm) was used to illuminate for 0, 5, 10, and 15 min, respectively. After 1 h, absorb an appropriate amount of supernatant and add it to a 96-well plate containing ATP detection working solution for measurement.

### 1.12. Antitumor and safety evaluation *in vivo*

The experiments involving mice were approved by the animal care and use committee of Shenzhen University (certificate number: SYXK2014-0140). Female BALB/c mice (4–5 weeks of age) were subcutaneously inoculated with $2 \times 10^6$ cells to establish 4T1 xenografts. When the tumor sizes reached 50–100 $mm^3$, the tumor-bearing BALB/c mice were randomly divided into four groups to receive different treatments: PBS, PBS plus light, **Ru1**, and **Ru1** plus light. The mice were intratumorally injected with PBS or **Ru1** (5 mg $kg^{-1}$) on days 0, 2, and 4, and the mice of light groups were irradiated with a 450 nm laser (15 mW $cm^{-2}$) for 15 min. The volumes of the transplanted tumors were measured every 2 days and calculated according to the formula $V = ab^2 \times 0.5$, where $a$ and $b$ were the longest and shortest diameters of the tumors, respectively. After the treatment, the organs of the mice were collected and fixed with 4% paraformaldehyde at 4 °C. The samples were then transferred to 10% formalin solutions and embedded in paraffin. After staining with H&E, the sections were examined under a Zeiss inverted fluorescence microscope.

### 1.13. Detection of tumor immunity in mice by flow cytometry

In order to systematically study the anti-tumor immunity of immune cells *in vivo*, antibody staining analysis of immune cells was performed by flow cytometry. Take the tumor (half of the tissue) and lymph nodes of the mouse, digest the tissue with 1 mg/mL collagenase IV and 0.1 mg/mL DNase I, and then filter the single-cell suspension through a 70 μm nylon cell filter. After removal with erythrocyte lysis buffer, we stained the obtained dendritic cells with anti-CD80-mouse-APC and anti-CD86-mouse-PE, while T lymphocytes were stained with anti-CD8-mouse-APC and anti- CD4-mouse-FITC was used for staining, and finally detected and analyzed by flow cytometry.

**1.14. Immunohistochemical detection of tumor immunity in mice**

Mouse tumor tissue (half of the tissue) was taken and fixed with 10% buffered formalin. The formalin was then removed with 75% ethanol, followed by dehydration, embedding, and sectioning. Sections were re-deparaffinized with xylene and dehydrated again with different concentrations of ethanol. The antigen is subsequently exposed by heat. Block with 5% bovine serum albumin for 1 h. After blocking, CD4, CD8, and γ-H2A.X primary antibodies were added and incubated overnight in a 4-degree refrigerator. After incubation, wash with PBS, then add HRP secondary antibody and incubate at room temperature for 1 hour. After incubation, wash with PBS, and then add DAB color development solution. After the color development is completed, wash and add hematoxylin for nuclear staining, then PBS (pH7.4) reverses the blue, and finally dehydrates and transparently mounts the slides.

**1.15. Statistical analysis**

All the experiments were replicated and the specific number of replicates done was either annotated in the figure legends or the specific section. Unless otherwise specified, the statistical significance of this study is determined by the unpaired, two-tailed Student's t-test at $*p < 0.05$ and $**p < 0.01$. Data were presented as means ± standard deviations (SD).

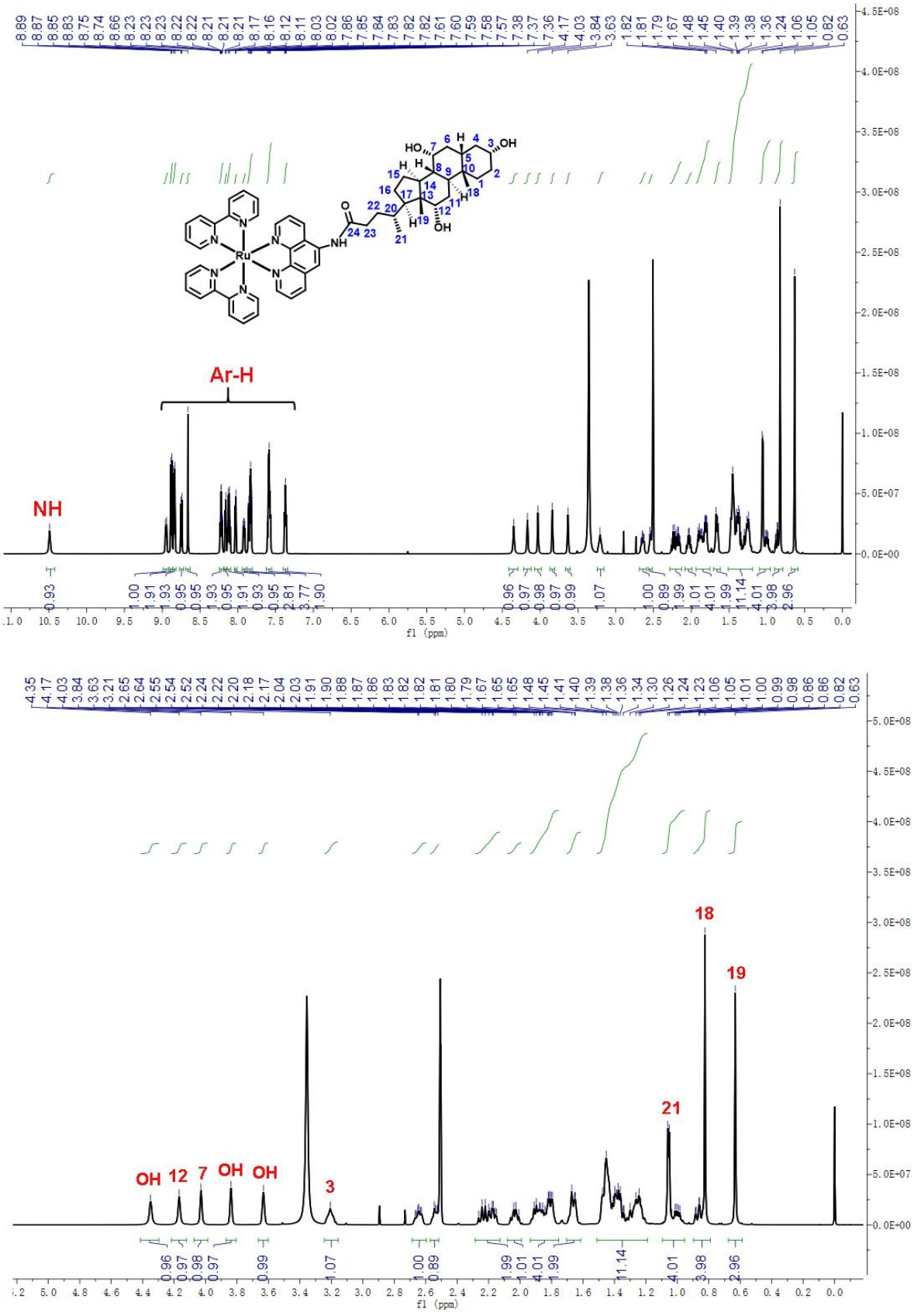


**Fig. S1.** $^{1}$H NMR spectrum of complex **Ru1**.

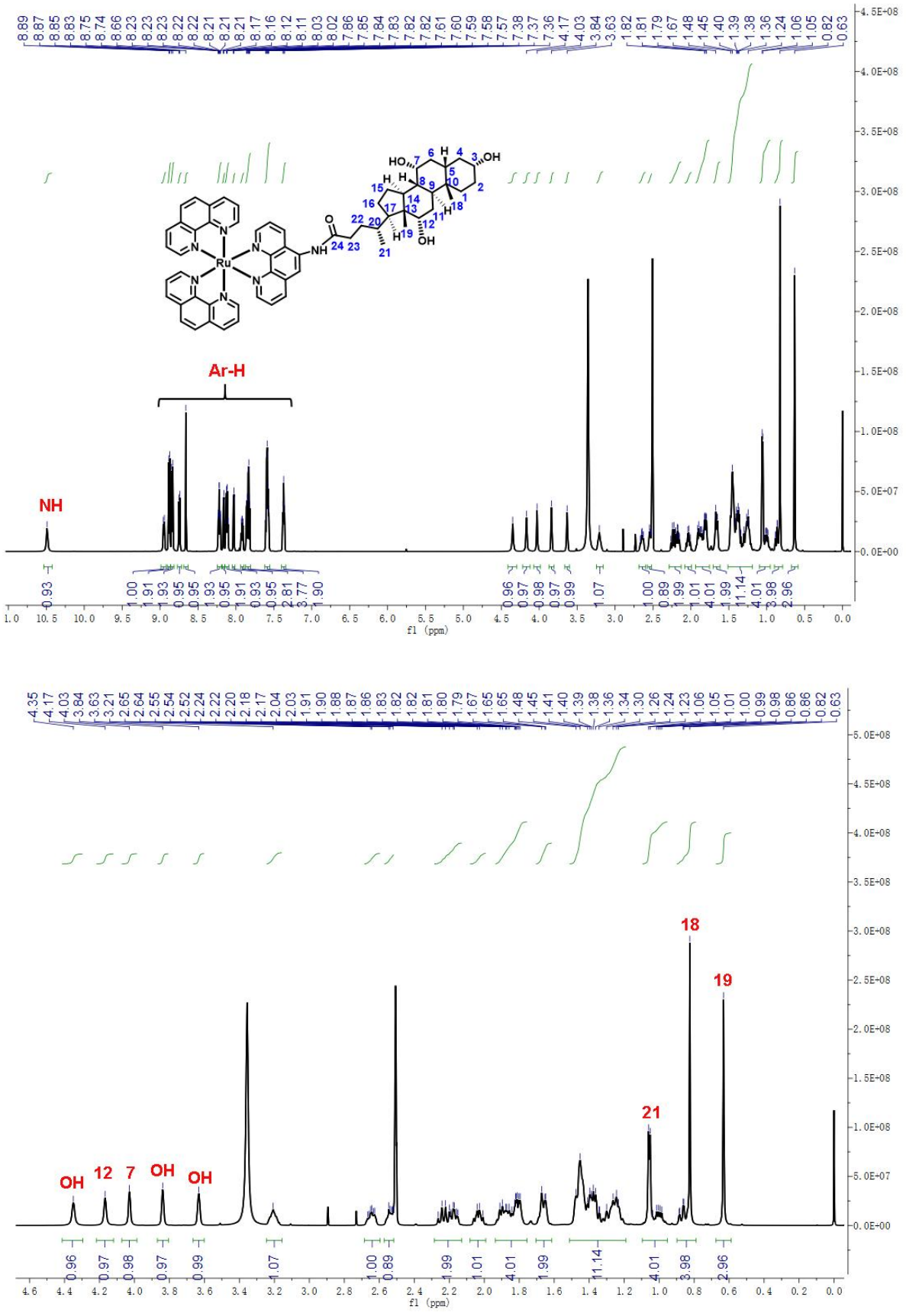


**Fig. S2.** $^{1}$H NMR spectrum of complex **Ru2**.

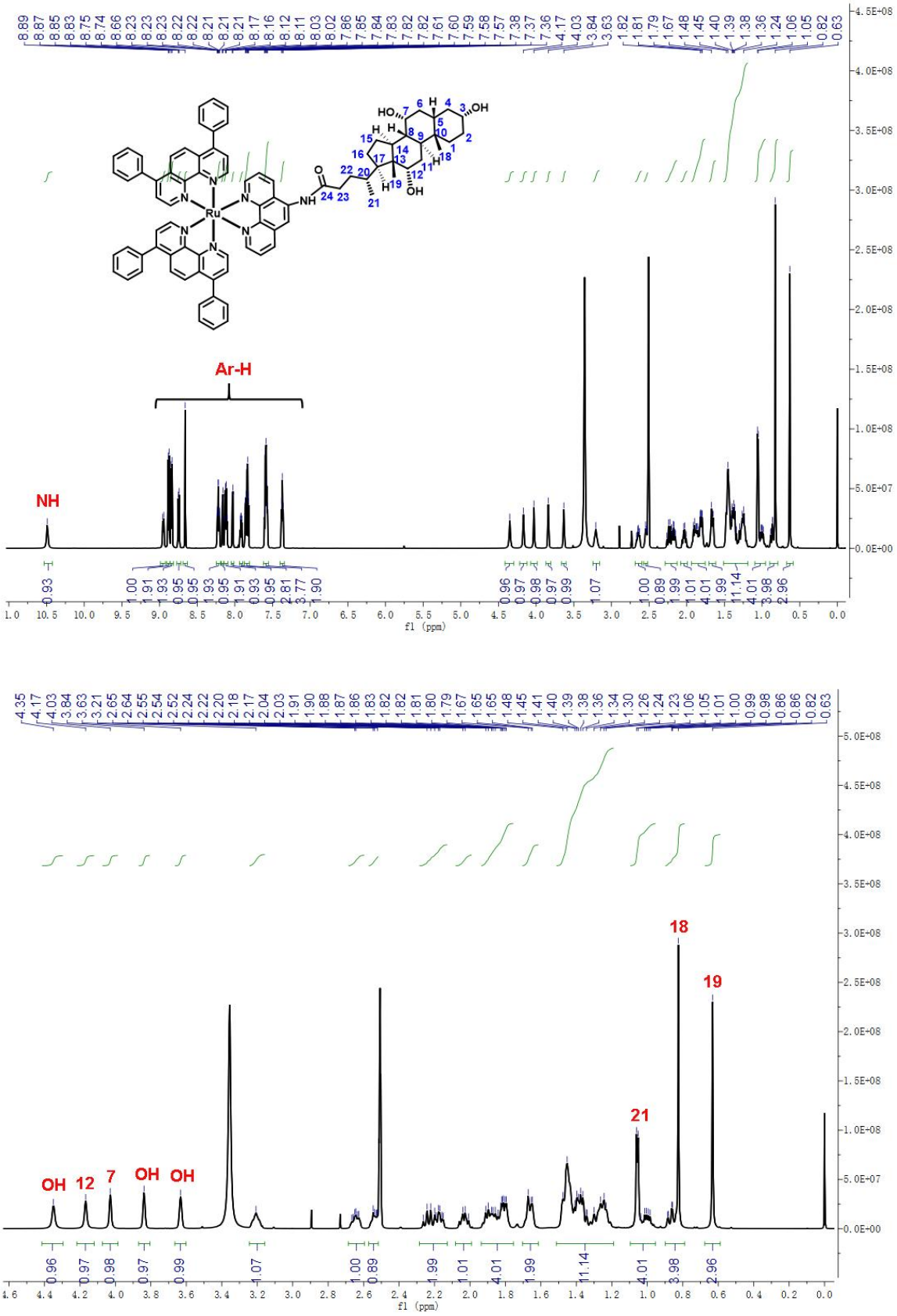


**Fig. S3.** $^{1}$H NMR spectrum of complex **Ru3**.

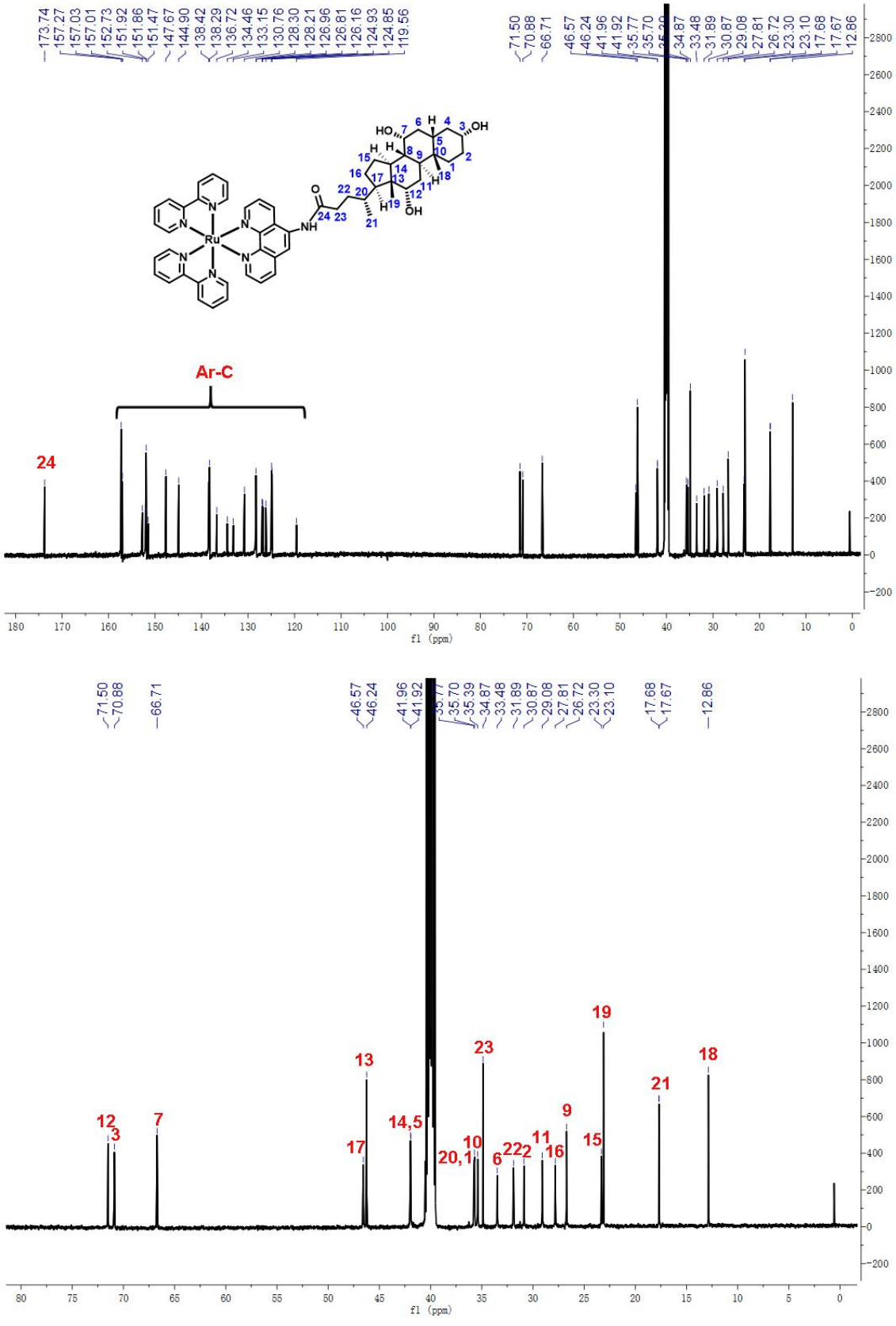


**Fig. S4.** $^{13}C$ NMR spectrum of complex **Ru1**.

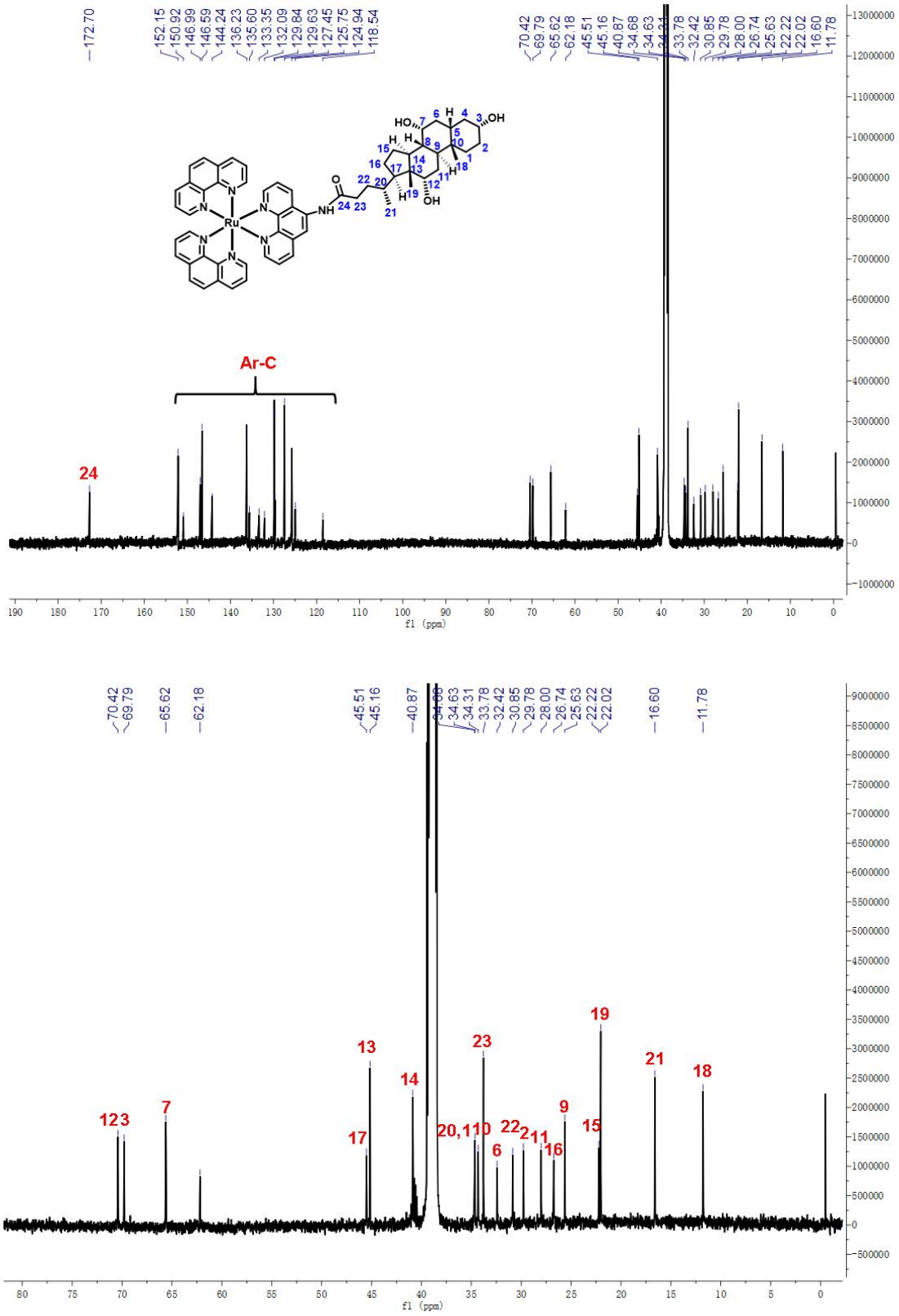


**Fig. S5**. $^{13}C$ NMR spectrum of complex **Ru2**.

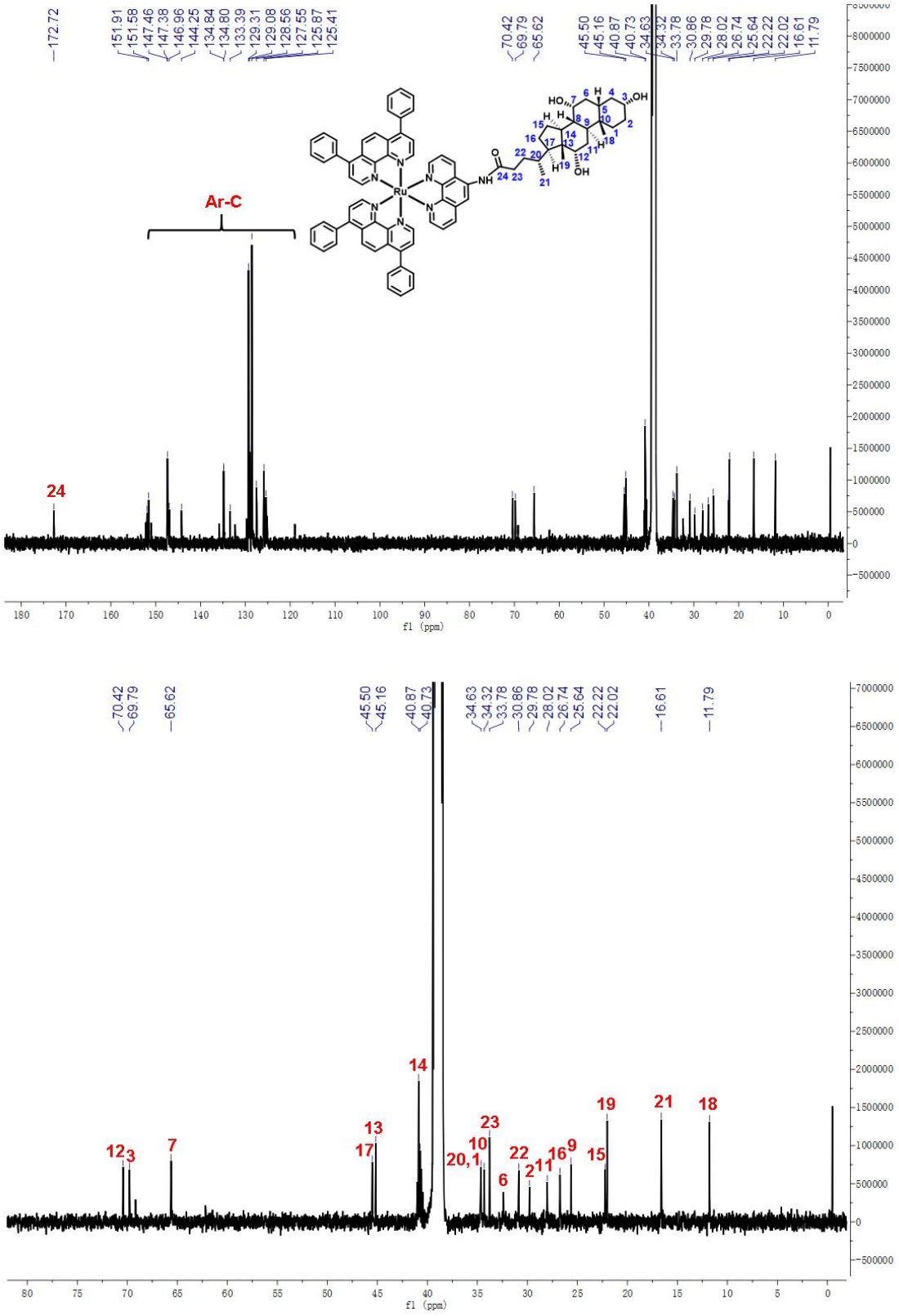


**Fig. S6**. $^{13}C$ NMR spectrum of complex **Ru3**.

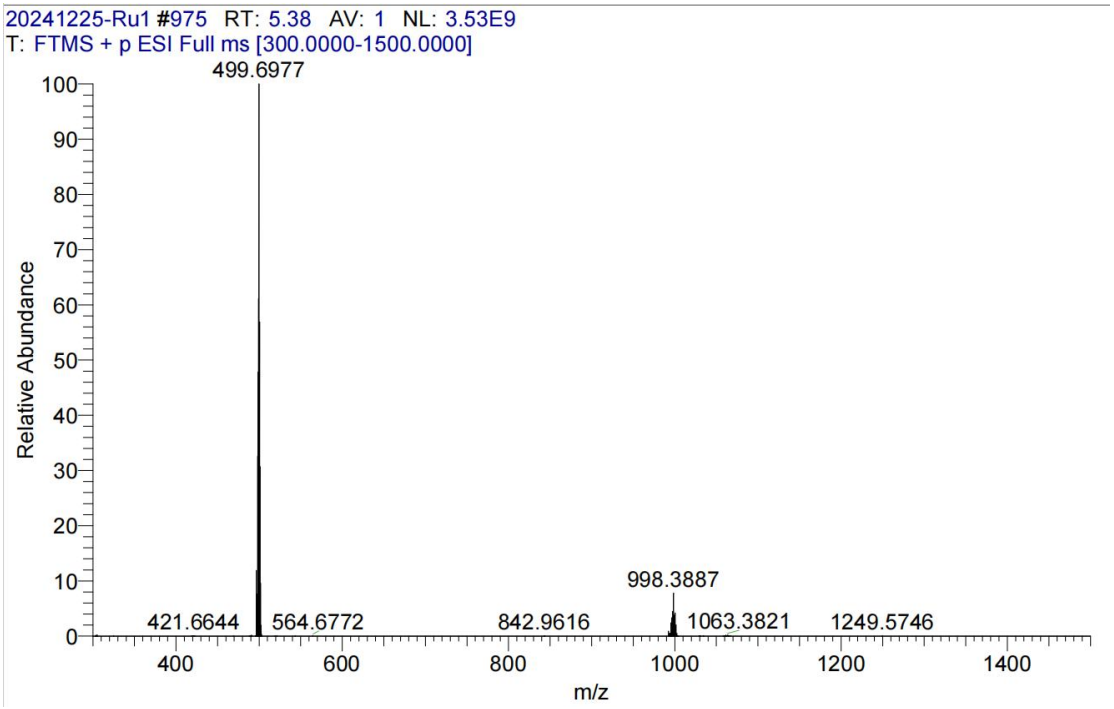


**Fig. S7**. ESI-MS spectrum of complex **Ru1** in methanol. $[M-2PF_6]^{2+}$, 499.6977.

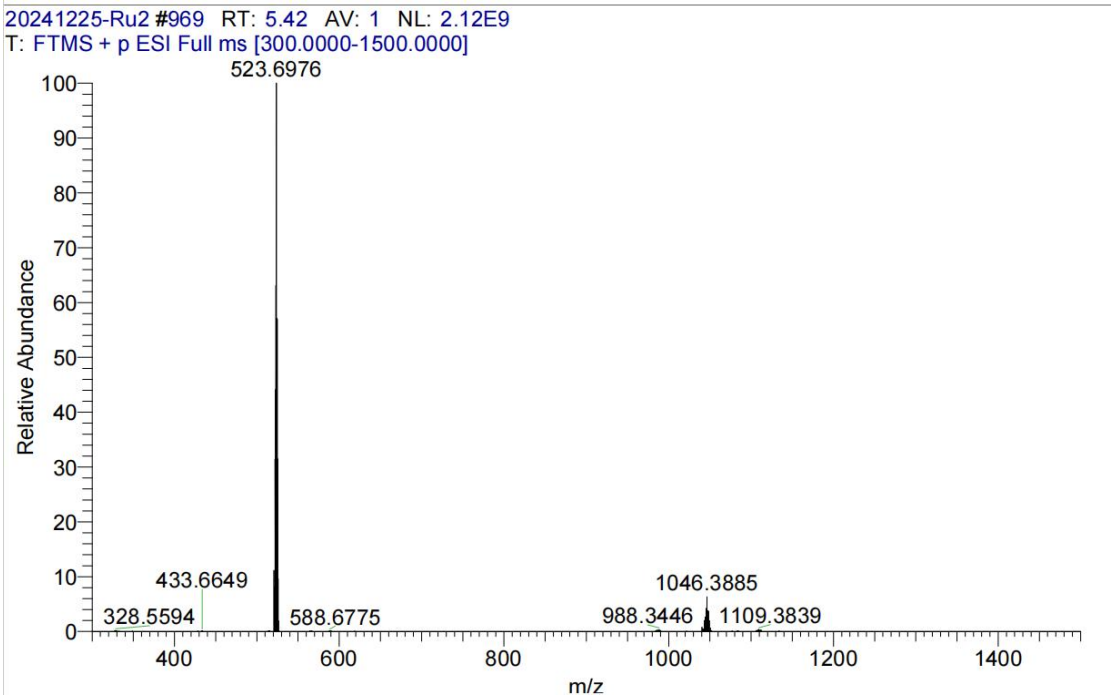


**Fig. S8**. ESI-MS spectrum of complex **Ru2** in methanol. $[M-2PF_6]^{2+}$, 523.6976.

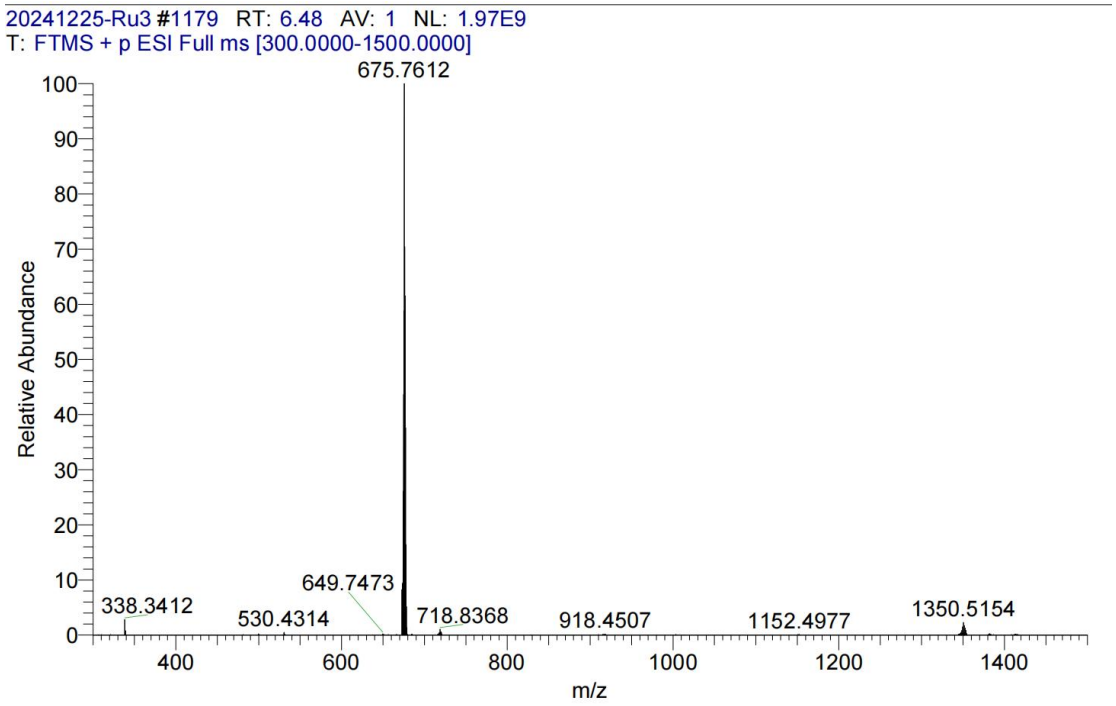


**Fig. S9**. ESI-MS spectrum of complex **Ru3** in methanol. $[M-2PF_6]^{2+}$, 675.7612.

==== Shimadzu LabSolutions Analysis Report ====

| | | | |
|---|---|---|---|
| Sample Name | : Ru1 | | |
| Sample ID | : | | |
| Data Filename | : Ru1.lcd | | |
| Method Filename | : MEOH-30min.lcm | | |
| Batch Filename | : 20241220.lcb | | |
| Vial # | : 1-1 | | |
| Injection Volume | : 30 uL | | |
| Date Acquired | : 2024/ 12/20 17:10:15 | Acquired by | : System Administrator |
| Date Processed | : 2024/ 12/20 19:48:32 | Processed by | : System Administrator |

<Chromatogram

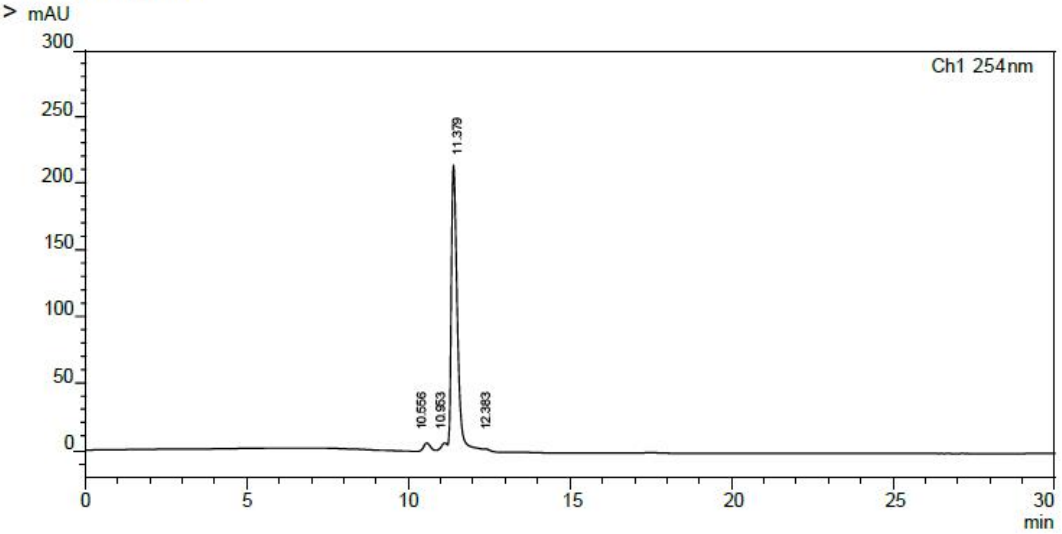


<Peak Table>

Ch1 254nm

| Peak# | Ret. Time | Area | Height | Conc. | Unit | Mark | Name |
|---|---|---|---|---|---|---|---|
| 1 | 10.556 | 13122 | 863 | 1.729 | | | |
| 2 | 10.953 | 3536 | 247 | 0.466 | | V | |
| 3 | 11.379 | 740903 | 57460 | 97.635 | | SV | |
| 4 | 12.383 | 1289 | 98 | 0.170 | | T | |
| Sum | | 758850 | 58668 | | | | |

**Fig. S10**. The purity of **Ru1** determined by HPLC.

==== Shimadzu LabSolutions Analysis Report ====

| | | | |
|---|---|---|---|
| Sample Name | : Ru2 | | |
| Sample ID | : | | |
| Data Filename | : Ru2.lcd | | |
| Method Filename | : MEOH30min.lcm | | |
| Batch Filename | : 20241220.lcb | | |
| Vial # | : 1-2 | | |
| Injection Volume | : 30 uL | | |
| Date Acquired | : 2024/12/20 17:50:45 | Acquired by | : System Administrator |
| Date Processed | : 2024/12/20 20:00:27 | Processed by | : System Administrator |

<Chromatogram>

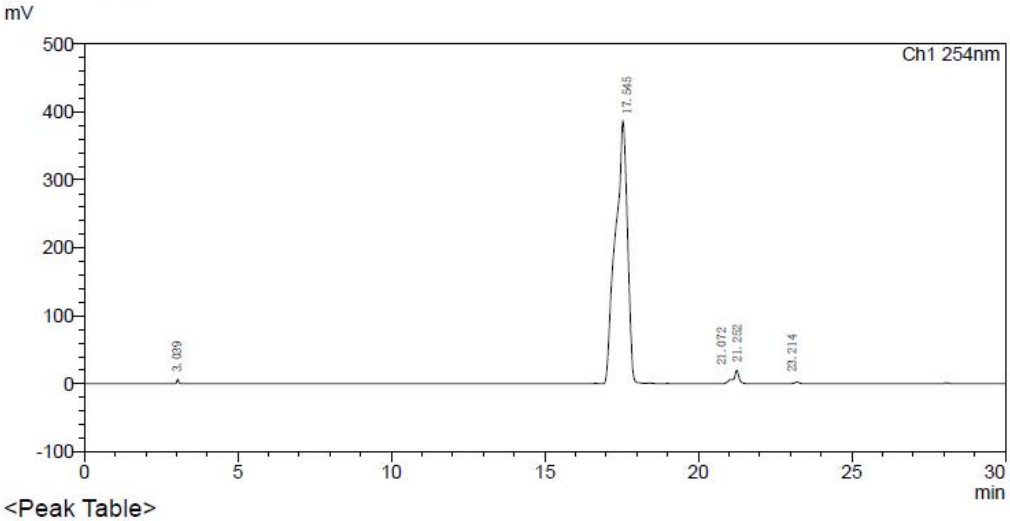


<Peak Table>

Ch1 254 nm

| Peak# | Ret. Time | Area | Height | Conc. | Unit | Mark | Name |
|---|---|---|---|---|---|---|---|
| 1 | 3.039 | 28227 | 6236 | 0.257 | | V | |
| 2 | 17.545 | 10641169 | 386599 | 96.937 | | SV | |
| 3 | 21.072 | 70402 | 6346 | 0.641 | | TV | |
| 4 | 21.252 | 206103 | 20943 | 1.878 | | TV | |
| 5 | 23.214 | 31560 | 2600 | 0.288 | | TV | |
| Sum | | 10977462 | 422724 | | | | |

**Fig. S11**. The purity of **Ru2** determined by HPLC.

==== Shimadzu LabSolutions Analysis Report ====

| | | | |
|---|---|---|---|
| Sample Name | : Ru3 | | |
| Sample ID | : | | |
| Data Filename | : Ru3.lcd | | |
| Method Filename | : MEOH.lcm | | |
| Batch Filename | : 20241221.lcb | | |
| Vial # | : 1 | | |
| Injection Volume | : 10 uL | | |
| Date Acquired | : 2024/12/21 18:00:06 | Acquired by | : System Administrator |
| Date Processed | : 2024/12/21 23:07:46 | Processed by | : System Administrator |

<Chromatogram>

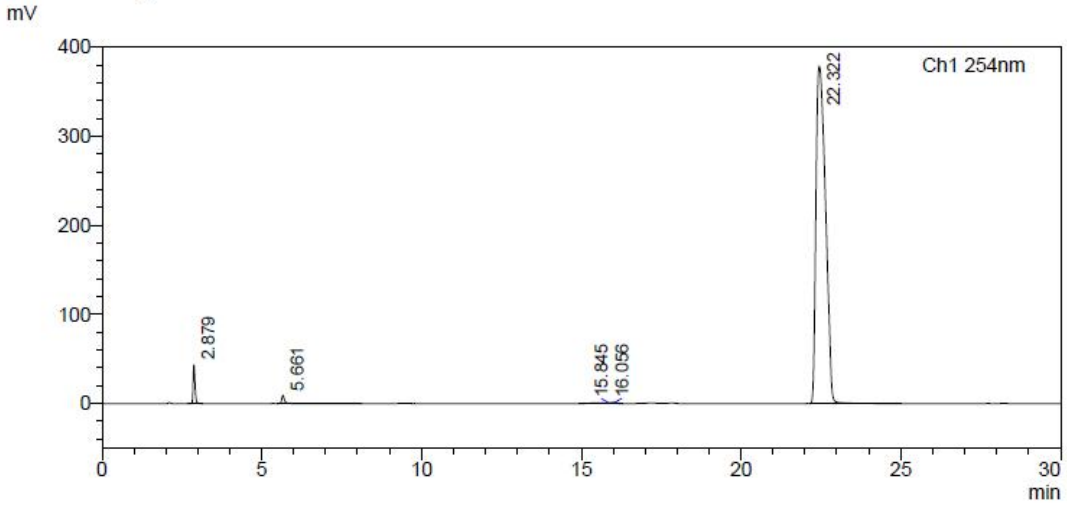


<Peak Table>

Ch1 254 nm

| Peak# | Ret. Time | Area | Height | Conc. | Unit | Mark | Name |
|---|---|---|---|---|---|---|---|
| 1 | 2.879 | 181363 | 43567 | 2.192 | | | |
| 2 | 5.661 | 61594 | 9233 | 0.744 | | SV | |
| 3 | 15.845 | 36161 | 1112 | 0.437 | | V | |
| 4 | 16.056 | 21094 | 1549 | 0.255 | | V | |
| 5 | 22.322 | 7973414 | 382067 | 96.371 | | SV | |
| Sum | | 8273627 | 438528 | | | | |

**Fig. S12**. The purity of **Ru3** determined by HPLC.

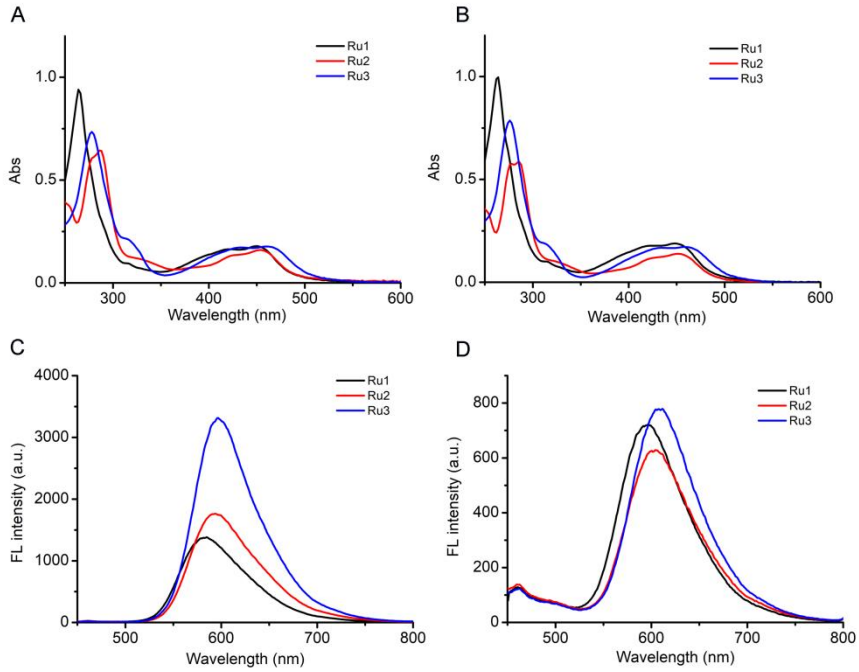


**Fig. S13**. (A, B) UV/Vis and (C, D) emission spectra of **Ru1**–**Ru3** ($2 \times 10^{-5}$ M) measured in DCM and MeCN at 298 K.

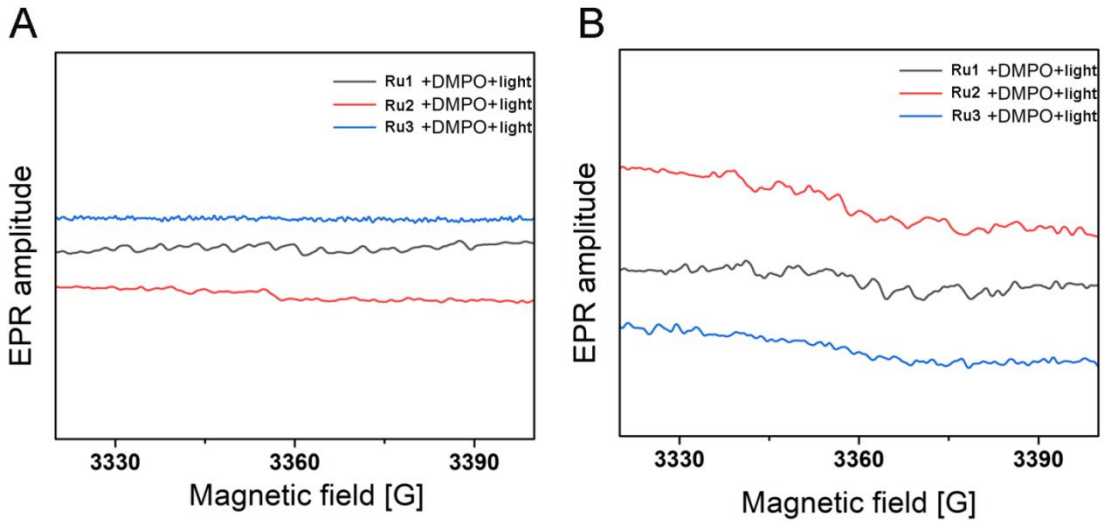


**Fig. S14**.The ESR spectra of $^{\bullet}OH$ and $O_2^{\bullet-}$ trapped by 5,5-dietyl-1-pyrroline N-oxide (DMPO) in different groups.

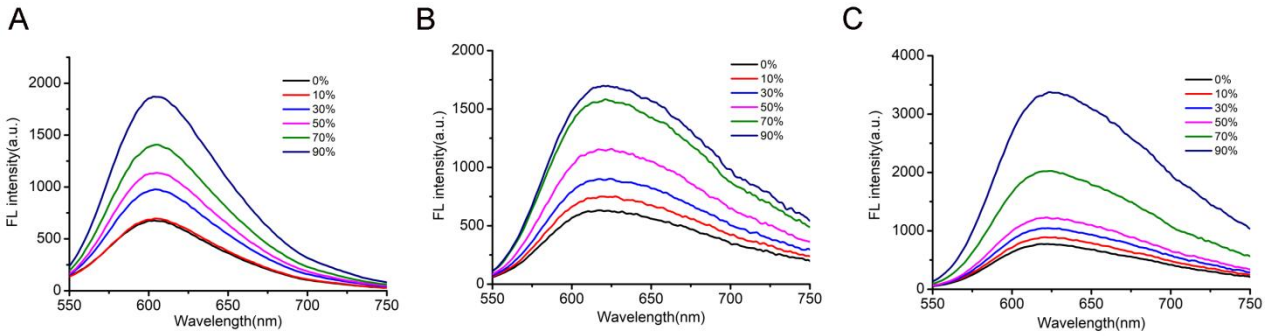


**Fig. S15**. (A, B, C) Fluorescence emission spectra of **Ru1**–**Ru3** (3 μM) at the mixing ratio of $H_2O/CH_3CN$ (0–90%, v/v).

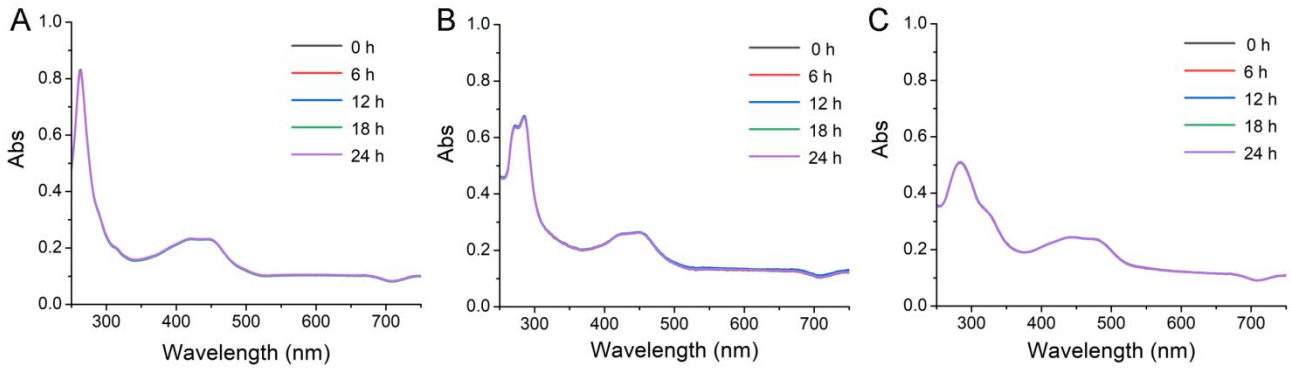


**Fig. S16.** Stability determination of **Ru1**–**Ru3** (20 μM) in PBS.

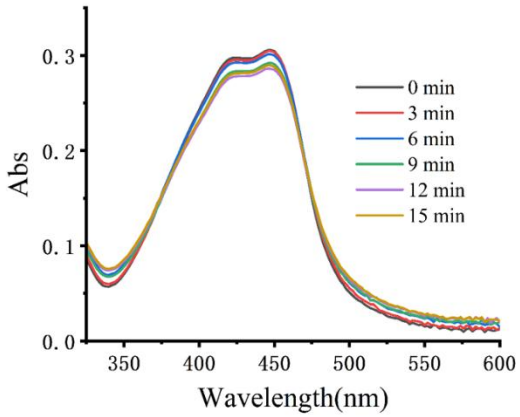


**Fig. S17.** Photostability determination of **Ru1** (20 μM) in PBS.

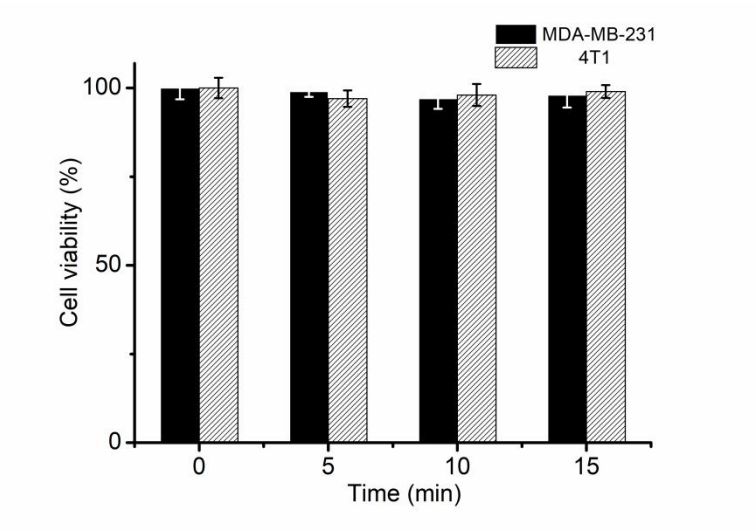


**Fig. S18.** The viability of MDA-MB-231 and 4T1 cells after light irradiation for 0,5,10 and 15 min.

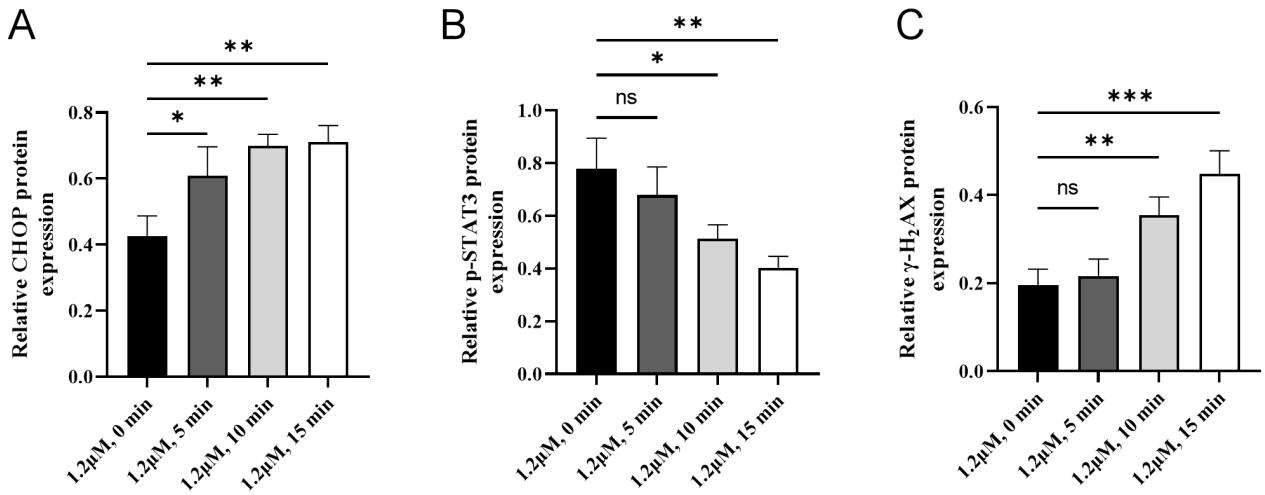


**Fig. S19.** Quantitative analysis of CHOP (A), p-STAT3 (B) and γ-H2AX (C) protein expression after treatment in Fig. 3B. Data are shown as mean ± SD, n=3. *p < 0.05, **p < 0.01, ***p < 0.001.

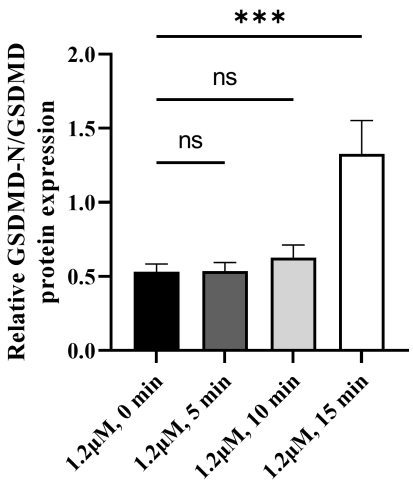


**Fig. S20.** Quantitative analysis of cleaved/full GSDMD protein expression after treatment in Fig. 4C. Data are shown as mean ± SD, n=3. ***p < 0.001.

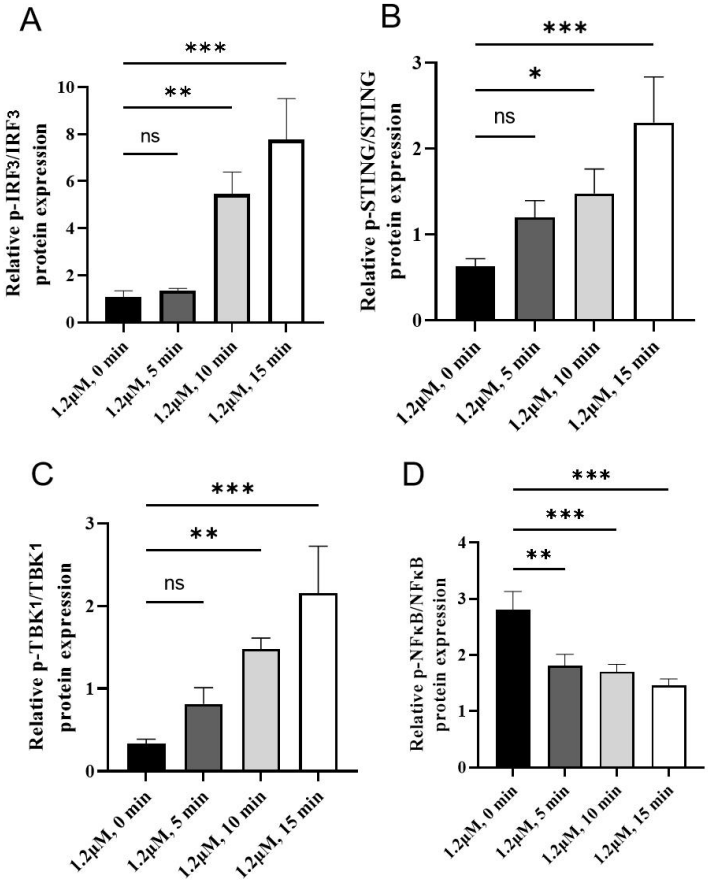


**Fig. S21**. Quantitative analysis of phosphorylation/full $IRF_3$ (A), STING (B), $TBK_1$ (C), NFκB (D) protein expression after treatment in (a). Data are shown as mean ± SD, n=3. *p < 0.05, **p < 0.01, ***p < 0.001.

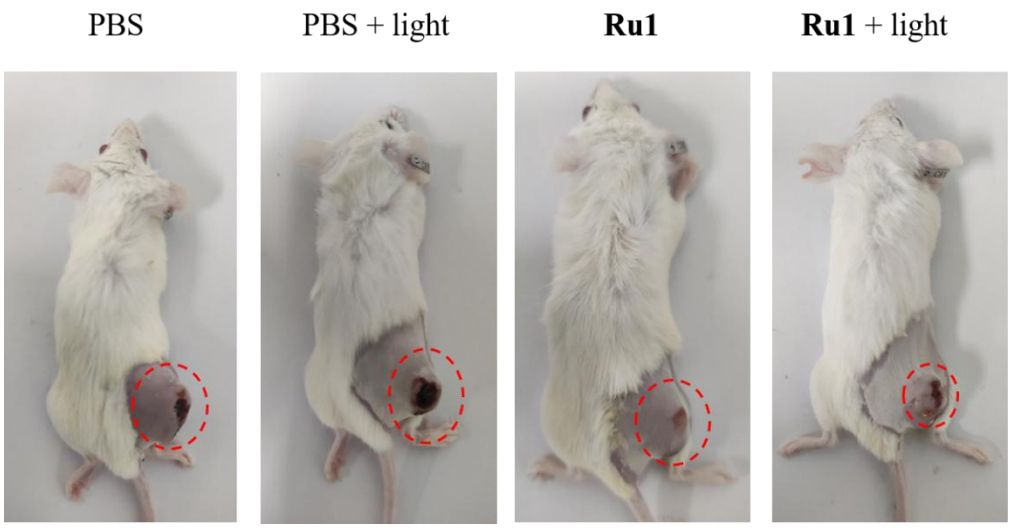


**Fig. S22.** Photos of Balb/c mice after PDT.

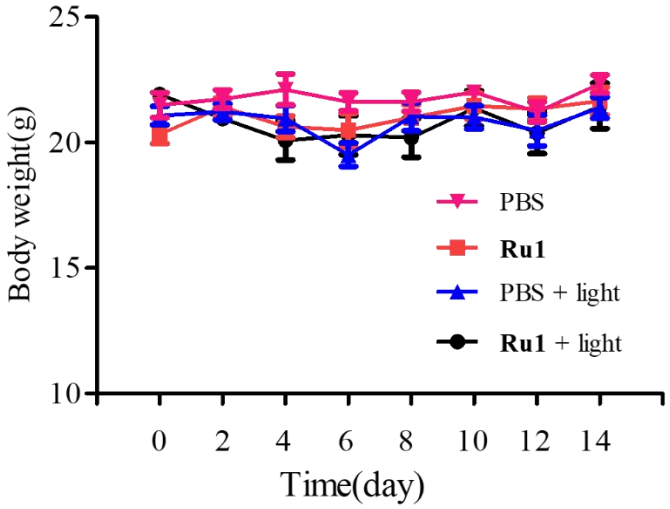


**Fig. S23**. Effect of complex **Ru1** on body weight of mice

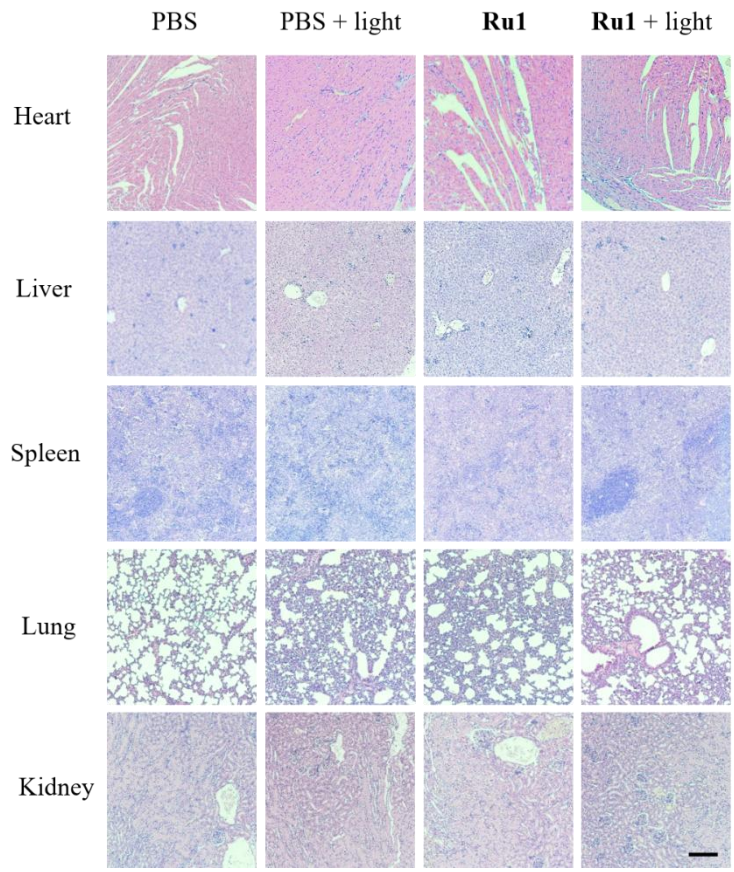


**Fig. S24.** Hematoxylin-eosin (H&E) staining of organs separated from nude mice after treatment with PBS, PBS + light, **Ru1** (5 mg/kg) and **Ru1** (5 mg/kg) + light. Scale bar: 50 μm.

**References**

1. T. J.Meyer, J. B.Godwin, Preparation of ruthenium nitrosyl complexes containing 2,2'-bipyridine and 1,10-phenanthroline. *Inorg. Chem.*, 1971, **10**, 471-474.
2. R. M. Hartshorn and J. K. Barton, Novel dipyridophenazine complexes of ruthenium(II): exploring luminescent reporters of DNA. *J. Am. Chem. Soc.*, 1992, **114** , 5919 -5925.
3. C. A. Puckett and J. K. Barton, Mechanism of cellular uptake of a ruthenium polypyridyl complex. *Biochemistry*, 2008, **47**, 11711-11716.
4. X. Xu, M. Chen, S. Jiang, Z. Pan, C. Zhao, Endoplasmic Reticulum-Targeting Iridium(III) Nanosonosensitizer Amplifies Immunogenic Cell Death for Boosted Tumor Sono-Immunotherapy, *Adv. Funct. Mater.*, 2024, **26** ,2314780.
5. Y. Zheng, W. J. Wang, J. X. Chen, K. Peng, X. X. Chen, Q. H. Shen, B. B. Liang, Z. W. Mao, C. P. Tan, Ruthenium(II) Lipid-Mimics Drive Lipid Phase Separation to Arouse Autophagy-Ferroptosis Cascade for Photoimmunotherapy. *Adv. Sci.*, 2024, e2411629.